Classical phase synchronization in dissipative non-Hermitian coupled systems

Jonas Rohn,[1,2] Kai Phillip Schmidt,[2] and Claudiu Genes[1,2]
[1]*Max Planck Institute for the Science of Light, Staudtstraße 2, D-91058 Erlangen, Germany*
[2]*Department of physics, University of Erlangen-Nuremberg, Staudtstraße 7, D-91058 Erlangen, Germany*

(Received 23 January 2022; revised 26 May 2023; accepted 8 August 2023; published 22 August 2023)

We study the interplay between non-Hermitian dynamics and classical phase synchronization in a system of $\mathcal{N}$ bosonic modes commonly coupled to an auxiliary, driven mode. For any set of non-Hermitian bipartite interactions between the auxiliary and other modes, the system evolves towards a phase synchronized state. We provide analytical and numerical evidence of such classical phase synchronization for systems ranging from a few modes to the macroscopic limit of large $\mathcal{N}$ and analyze the effects of inhomogeneous frequency broadening and robustness under the action of external thermal noise.

DOI: 10.1103/PhysRevA.108.023721

I. INTRODUCTION

Synchronization has a wide relevance in a variety of disciplines ranging from biology to neuroscience, electrical engineering, mathematics, and physics, and it originates from Huygens' observation a few centuries back [1–6]. In 1975 Kuramoto introduced the *Kuramoto model* [5–7] to show the emergence of phase synchronization in multiple self-sustained oscillators with mutual, nonlinear couplings. The basis of the model entails that the time derivative of the phase ϕ_i of the ith oscillator is given by its frequency ω_i and an additional nonlinear interaction term that induces all $\mathcal{N}$ phases to approximately converge, provided its strength K is sufficiently large. Mathematically, this is formulated as $\dot{\phi}_i = \omega_i + K/\mathcal{N}\sum_{j=1}^{\mathcal{N}} \sin(\phi_j - \phi_i)$. Kuramoto's solution in the macroscopic limit provides an analytical estimate of the (identical) coupling strengths for the synchronization threshold. Nowadays, several variations of the original model are known, including the study of modified couplings such as the Sakaguchi-Kuramoto model, where a constant phase shift is added to the nonlinear interaction term, driving terms, and other types of network topologies representing the mutual oscillator couplings [8–10]. The coexistence of synchronized and desynchronized domains, so-called chimera states, has been investigated [11] and shown to be analytically solvable [12], also in the presence of noise [13].

The emerging field of non-Hermitian physics recently aroused great interest [14–17] and has already found experimental implementations, such as in microwave optomechanical circuits or cavity optomagnonics[18]. Other promising platforms realizing non-Hermitian Hamiltonians can be found in several subdisciplines [15], for example, in the realm of classical electric circuits [19] or in optical setups [20,21]. The suggested procedure for obtaining non-Hermitian couplings is to eliminate auxiliary, lossy modes in otherwise Hermitian open systems such as applied in Ref. [22] to show the occurrence of exceptional points and level attraction or as proposed in Ref. [23] for the implementation of topological amplification in photonic lattices based on realizations motivated by experiments in superconducting circuit setups [24]. Non-Hermitian coupling of two modes of different frequencies leads to level attraction (the opposite of level repulsion, standard in strongly coupled systems), or pulling of the modes towards a common frequency: this is reminiscent of synchronization as already remarked in Ref. [22]. Therefore, we pose here a timely question: whether non-Hermitian interactions can be used as a resource for synchronization, even in the absence of an explicit nonlinear ingredient. To this end, we consider a system of $\mathcal{N}$ oscillators linearly coupled to a (possibly) driven auxiliary mode a_0 [see Fig. 1(a)] with interactions smoothly tunable from purely Hermitian to fully anti-Hermitian. We find that phase synchronization can be reached [see Figs. 1(b) and 1(c)] for identical oscillators and that it is indeed the non-Hermitian coupling that plays the main role in synchronization. As the system is described by a bilinear form Hamiltonian (albeit non-Hermitian) it allows fully analytical solutions; however, this linearity is apparent as it turns into an effective nonlinear coupling at the level of classical phases and it allows, via some mathematical manipulations, a mapping onto the standard Kuramoto model. Our approach is the following: (1) we provide numerical evidence of phase synchronization for $\mathcal{N}$ main oscillators coupled to an auxiliary, driven one, (2) we match numerical results with analytical predictions, and (3) we provide a transformation to a collective basis, where a Kuramoto-like model allows for the matching of the previously derived synchronization conditions to the Kuramoto predictions. Furthermore, we numerically test for robustness against external thermal noise and reveal resilience to noise in driven systems. Additionally, we discuss the effect of frequency disorder, stemming, for example, from inhomogeneous broadening; we find that low

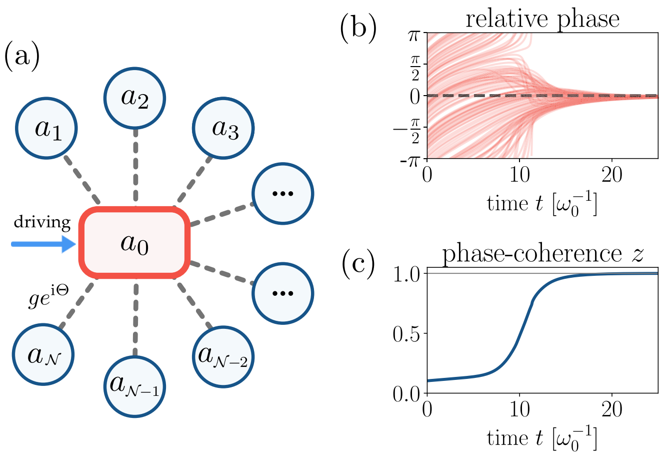

FIG. 1. (a) Setup showing a driven auxiliary mode a_0 coupled to $\mathcal{N}$ modes at rates $ge^{i\Theta}$. The tuning of Θ allows for a smooth transition from Hermitian to fully anti-Hermitian dynamics. (b) Convergence of the relative phases $\phi_j - \phi_0$ to zero for $\mathcal{N} = 100$ modes for full anti-Hermitian coupling. (c) The phase coherence $z = |\sum_j \exp(i\phi_j)|/\mathcal{N}$ (close to zero for the initially fully unsynchronized system) shows full synchronization ($z = 1$) for large times. Parameters are $\omega = 1.1$, $\omega_0 = 1.0$, $\gamma = 0.2$, $\gamma_0 = 0.1$, $g = 0.1$, $\Theta = 3/4\,\pi$, $\Omega = 0.9$, and $\eta = 0.5$.

disorder can be tolerated and that, past a certain threshold, the system synchronizes to two groups of opposing phases.

The paper is organized as follows: we introduce the model and equations in Sec. II and discuss their results in Sec. III showing the emergence of a phase synchronization regime reached via the tuning of a non-Hermitian parameter. In Sec. IV we then provide a transformation to a collective basis, where the couplings among oscillators resemble the well-known Kuramoto model. Finally, we provide numerical simulations in Sec. V, taking into account effects of disorder and thermal environment.

II. MODEL AND EQUATIONS

We consider a subsystem of $\mathcal{N}$ bosonic modes a_i, with $[a_i, a_j^\dagger] = \delta_{ij}$ at frequency ω, identically coupled to the (possibly) driven auxiliary mode a_0 oscillating at frequency ω_0, as sketched in Fig. 1(a). The oscillators are immersed in independent baths; the effect of the environment is included via the decay rate γ_0 with corresponding collapse operator a_0 for the auxiliary mode and identical rates γ and collapse operators a_i for all other modes. This is done using a standard Lindblad form

$$\mathcal{L}[\rho] = \gamma_{\mathcal{O}}[2\mathcal{O}\rho(t)\mathcal{O}^\dagger - \mathcal{O}^\dagger\mathcal{O}\rho(t) - \rho(t)\mathcal{O}^\dagger\mathcal{O}], \quad (1)$$

for any collapse operator $\mathcal{O}$ and collapse rate $\gamma_{\mathcal{O}}$ [25,26] and included in the master equation for the density operator ρ describing the time evolution of the system $\dot{\rho}(t) = i[\rho(t), \mathcal{H}_{\text{total}}] + \mathcal{L}[\rho]$. The total Hamiltonian contains the following contributions: $\mathcal{H}_{\text{total}} = \mathcal{H}_0 + \mathcal{H}_{\text{coupling}} + \mathcal{H}_{\text{drive}}$. The free part describes free evolution of the $N + 1$ bosonic modes:

$$\mathcal{H}_0 = \omega_0 a_0^\dagger a_0 + \sum_{i=1}^{\mathcal{N}} \omega a_i^\dagger a_i\,. \quad (2)$$

The coupling terms, generally assumed non-Hermitian, between the auxiliary mode and all other $\mathcal{N}$ modes are included in

$$\mathcal{H}_{\text{coupling}} = \frac{g}{\sqrt{\mathcal{N}}} e^{i\Theta} \sum_{i=1}^{\mathcal{N}} (a_0^\dagger a_i + a_0 a_i^\dagger). \quad (3)$$

While non-Hermitian dynamics is not straightforward to obtain, a simple example is illustrated in Appendix B, where it is seen as occurring in a bipartite system via coupling to an auxiliary, lossy third-party system, later eliminated from the dynamics. The drive term is $\mathcal{H}_{\text{drive}} = i\eta(a_0^\dagger e^{-i\Omega t} - a_0 e^{i\Omega t})$ where $\eta \in \mathbb{R}$ is the driving strength of a_0, Ω is the driving frequency and $g \in \mathbb{R}$ is the coupling strength (assumed identical for any mode i). Crucially, we allow the couplings to be non-Hermitian and characterized by the parameter $\Theta \in (-\pi, \pi]$. For $\Theta = 0$ or π the usual case of a Hermitian, coherent interaction is obtained, characterized by the possible occurrence of strong coupling physics (and subsequently level repulsion) whereas $\Theta = \pm\pi/2$ yields a fully anti-Hermitian coupling term leading to level attraction.

The evolution (in a frame rotating at the laser frequency) is followed at the level of classical amplitudes $\alpha_i := \langle a_i \rangle \in \mathbb{C}$. The equations of motion are derived from the master equation for the density operator ρ of the whole system, $\dot{\rho}(t) = i[\rho(t), \mathcal{H}_{\text{total}}] + \mathcal{L}[\rho]$ (where all Hamiltonian terms and loss channels are encompassed in $\mathcal{H}_{\text{total}}$ and $\mathcal{L}[\rho]$ terms) via $\dot{\alpha}_i = \text{Tr}[a_i\dot{\rho}]$ and can be cast in a compact form (see Appendix B) as

$$\dot{\mathbf{A}} = -i \underbrace{\begin{pmatrix} \delta_0 - i\gamma_0 & \frac{g}{\sqrt{\mathcal{N}}}e^{i\Theta} & \cdots & \frac{g}{\sqrt{\mathcal{N}}}e^{i\Theta} \\ \frac{g}{\sqrt{\mathcal{N}}}e^{i\Theta} & \delta - i\gamma & & \\ \vdots & & \ddots & \\ \frac{g}{\sqrt{\mathcal{N}}}e^{i\Theta} & & & \delta - i\gamma \end{pmatrix}}_{\mathcal{H}} \mathbf{A} + \eta\,\mathbf{u}, \quad (4)$$

where $\mathbf{A} = (\alpha_0, \alpha_1, \ldots, \alpha_{\mathcal{N}})^T$, the driving vector $\mathbf{u} := (1, 0, \ldots, 0)^T$, and the frequency detunings $\delta_0 = \omega_0 - \Omega$, $\delta = \omega - \Omega$. An alternative derivation, capable of taking into account the presence of input quantum noise, could be derived directly from the quantum master equation, via a transformation to a set of quantum Langevin equations [25,27]. However, as we are interested only in classical behavior, eventually under the presence of classical thermal noise corresponding to a thermal environment which dominates the smaller effects of zero point fluctuations, our approach is equivalent to an averaging over the quantum Langevin equations, which sees the zero-averaged noise terms drop out. This suffices for an exact description of the time evolution of average values as long as one is not concerned with the variance of the quantum operators.

Notice that the system follows a linear evolution allowing for analytical solutions of the above equations. The results are presented in Sec. III showing the possibility of phase-synchronized regimes tunable via the tuning of the non-Hermitian parameter. However, a one-directional transformation of the above equations into equations for real amplitudes and phases shows the similarity of this model to the Kuramoto model (for a simple presentation of the model see Appendix A), as detailed in Sec. IV.

III. PHASE SYNCHRONIZATION

In order to analytically and numerically ensure that the phase difference between two oscillators is 0 or π in the long-time limit, we require $\mathrm{Im}(\alpha_i/\alpha_j)|_{t\to\infty} = 0$. To further distinguish between synchronization (zero phase difference) and antisynchronization (phase difference of π) we require $\mathrm{Re}(\alpha_i/\alpha_j)|_{t\to\infty} > 0$. The task is to find values of Θ and driving frequency Ω that lead to phase synchronization of all oscillators, assuming that $\omega_0, \gamma_0, \omega, \gamma, g$ and η are given. In the undriven case ($\eta = 0$), as amplitudes eventually decay to zero in the steady-state limit, we consider synchronization to be reached only when the synchronization time τ_{sync} is smaller than the decay time τ_{dec}. To calculate the ratios α_i/α_j, Eq. (4) is solved by diagonalizing $\mathcal{H}$. A set of example trajectories are given in Fig. 1(b) showing the convergences of all phases to a common value. Equivalently, the phase coherence $z = |\sum_j \exp(i\phi_j)|/\mathcal{N}$ illustrated in Fig. 1(c) shows the onset of full synchronization as z reaches unity.

A. Undriven case

For $\eta = 0$, $g > 0$, a single eigenmode of the system survives which, in the long-time limit, leads to the ratios α_i/α_j becoming independent of the initial amplitudes and approaching a constant value (see Appendix C). With the conditions listed above for the amplitude ratios, one can obtain a synchronization condition

$$\tan\Theta = -\frac{\gamma - \gamma_0}{\omega - \omega_0} = -\frac{\Delta\gamma}{\Delta\omega} \tag{5}$$

combined with the requirement that $\Delta\gamma \sin\Theta < \Delta\omega \cos\Theta$ (see Appendix C). Interestingly, g does not play a role, whereas it is crucial that the interaction is non-Hermitian. In particular, for $\Delta\omega = 0$, $\Delta\gamma < 0$, one finds $\Theta = \pi/2$, demonstrating the necessity of non-Hermitian interactions. Surprisingly, the Hermitian case $\Theta = 0$ which could be obtained by choosing $\Delta\gamma = 0$, $\Delta\omega > 0$ practically does not lead to synchronization since τ_{sync} diverges; cf. Fig. 2. Calling the system synchronized is sensible only unless τ_{sync} does not exceed the decay time τ_{dec} of the system. We find numerically from a simulation of Eq. (4) that $\tau_{\mathrm{sync}}^{-1}$ scales as $g\sin\Theta$ whereas $\tau_{\mathrm{dec}} = 1/\gamma$ (see Fig. 2).

B. Driven case

The situation is different for $\eta > 0$, where by a proper choice of Θ and Ω the synchronization condition (see Appendix C) reads instead

$$\tan\Theta = -\frac{\gamma}{\omega - \Omega}. \tag{6}$$

Combined with the condition $(\omega - \Omega)\cos\Theta < \gamma \sin\Theta$ it follows that phases coincide as soon as the oscillators enter the steady state. The driving strength η determines the steady-state amplitudes and the synchronization time τ_{sync}, but similar to g, it does not appear in the synchronization condition. One finds numerically that the synchronization time diverges in the Hermitian case $\Theta = 0$ as for the undriven case.

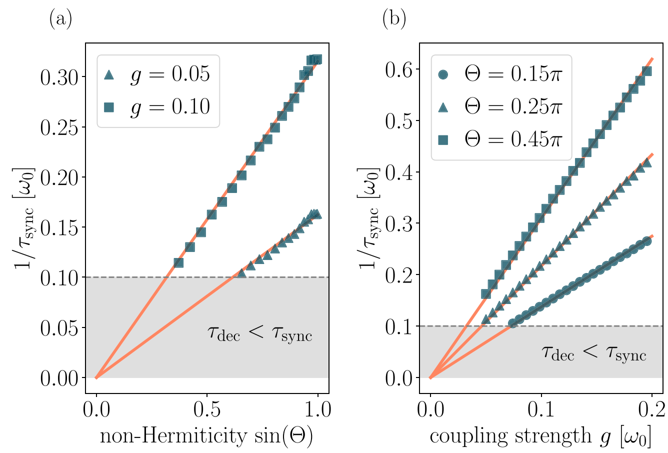

FIG. 2. Inverse mean synchronization time $\tau_{\mathrm{sync}}^{-1}$ as a function of (a) the non-Hermiticity parameter $\sin(\Theta)$ and (b) the coupling strength g. Here τ_{sync} is numerically estimated by averaging the time by which phases deviate from the auxiliary mode phase ϕ_0 not more than 0.05π. Linear lines are fits through the data points shown as symbols. Parameters are $\gamma = 0.1$, $\gamma_0 = 0.05$, $\omega_0 = 1.0$, and ω is chosen to satisfy the synchronization condition.

IV. MAPPING ONTO THE KURAMOTO MODEL

Let us now obtain a bit more insight into the synchronization behavior by crossing into the known model of nonlinear couplings known as the Kuramoto model.

A. Phase evolution

While Eq. (4) show linear evolution at the level of complex-valued amplitudes, the dynamics of phases $\phi_i = \arg\alpha_i$ and real-valued amplitudes $r_i = |\alpha_i|$ is described by the coupled evolution of $2(\mathcal{N}+1)$ nonlinear differential equations

$$\dot{r}_i = -\gamma_i r_i + \frac{g}{\sqrt{\mathcal{N}}}\sum_{j=1}^{\mathcal{N}} \zeta_{i,j}\sin(\Theta + \phi_j - \phi_i) r_j + \eta\delta_{i,0}\cos\phi_i,$$

$$\dot{\phi}_i = -\delta_i - \frac{g}{\sqrt{\mathcal{N}}}\sum_{j=1}^{\mathcal{N}} \zeta_{i,j}\frac{r_j}{r_i}\cos(\Theta + \phi_j - \phi_i) - \eta\delta_{i,0}\sin\phi_i, \tag{7}$$

where all the couplings and decay rates are defined in simplified form as $\zeta_{0,j} = 1 - \delta_{0,j}$, $\zeta_{i>0,j} = \delta_{i,j}$, $\delta_i = \delta_{i,0}\delta_0 + (1 - \delta_{i,0})\delta$, and $\gamma_i = \delta_{i,0}\gamma_0 + (1 - \delta_{i,0})\gamma$. Assuming an initial random distribution of all phases ϕ_j between 0 and 2π for $t = 0$, synchronization is then found if all phase differences approach zero, i.e., if $\phi_i(t) \approx \phi_j(t), \forall i, j \in \{0, \dots, \mathcal{N}\}$ for times $t > \tau_{\mathrm{sync}}$, where τ_{sync} denotes an estimate of the synchronization time. This is illustrated in Fig. 1. While the equations of motion are nonlinear, a direct connection to the Kuramoto model is not yet obvious but can instead be obtained in a collective basis as described in the following.

B. An effective Kuramoto model

The all-to-all coupling limit characterizing a standard Kuramoto model can be reproduced within a reduced subspace of dimension $\mathcal{N}$ comprising a set of collective modes

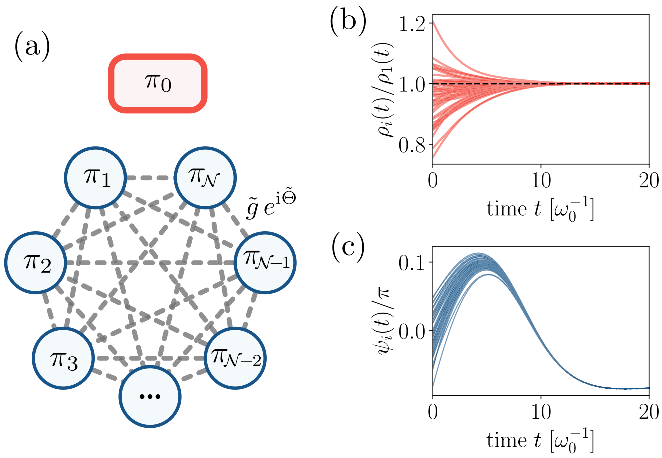

FIG. 3. (a) Setup showing $\mathcal{N}$ Kuramoto modes and the isolated eigenmode in a collective basis. (b) Time dynamics of ρ_i/ρ_1 converging to the decoupling region of unity. (c) Phases ψ_i (in the rotating frame) of the Kuramoto modes, starting to follow the dynamics of the driven Sakaguchi-Kuramoto model roughly around the region where amplitude ratios approach unity 1. Parameters are $\mathcal{N}=50$, $\omega_0=1.0$, $\omega=1.2$, $\gamma_0=0.25$, $\gamma=0.5$, $g=0.05$, $\Theta=\pi/2$, $\Omega=1.2$, and $\eta=0.1$.

obtained by the action of a linear mapping $\mathcal{U}$ (see Appendix C). This *collective basis* consists of $\mathcal{N}$ Kuramoto modes, equally coupled to each other and an isolated eigenmode [see illustration in Fig. 3(a)].

In this basis the equation of motion for the transformed complex amplitudes $\mathbf{P}=(\pi_0,\pi_1,\dots,\pi_\mathcal{N})^T:=\mathcal{U}\mathbf{A}$ reads $\dot{\mathbf{P}}=-i\mathcal{M}\mathbf{P}+\eta\tilde{\mathbf{u}}$ with an effective driving vector $\tilde{\mathbf{u}}=\mathcal{U}\mathbf{u}$ and the evolution matrix $\mathcal{M}=\mathcal{U}\mathcal{H}\mathcal{U}^{-1}$ is

$$\mathcal{M}=\begin{pmatrix}\tilde{\delta}_0-i\tilde{\gamma}_0 & 0 & 0 & \dots\\ 0 & \tilde{\delta}-i\tilde{\gamma} & \frac{\tilde{g}}{\mathcal{N}}e^{i\tilde{\Theta}} & \dots\\ 0 & \frac{\tilde{g}}{\mathcal{N}}e^{i\tilde{\Theta}} & \tilde{\delta}-i\tilde{\gamma} & \\ \vdots & \vdots & & \ddots\end{pmatrix}. \qquad (8)$$

The matrix shows that one collective mode gets decoupled from the other $\mathcal{N}$ collective modes, which instead undergo an all-to-all coupling dynamics. This is depicted in Fig. 3(a). The renormalized couplings are obtained as

$$\tilde{g}e^{i\tilde{\Theta}}=\tfrac{1}{2}(\Delta\omega-i\Delta\gamma\mp2\mu) \qquad (9)$$

with

$$\mu=\sqrt{(\Delta\omega-i\Delta\gamma)^2/4+g^2e^{2i\Theta}}. \qquad (10)$$

The detunings and decay rates are also redefined as

$$\tilde{\delta}_0-i\tilde{\gamma}_0=[(\delta+\delta_0)-i(\gamma+\gamma_0)]/2\pm\mu, \qquad (11a)$$

$$\tilde{\delta}-i\tilde{\gamma}=\delta-i\gamma+(\Delta\omega-i\Delta\gamma\mp2\mu)/(2\mathcal{N}). \qquad (11b)$$

In the following we assume that $\mathcal{U}$ always isolates the eigenmode with the fastest decay rate, which is always possible.

With the phases $\psi_i:=\arg\pi_i$ and real-valued amplitudes $\rho_i=|\pi_i|$ in the collective basis, one finds that ψ_0 increases linearly with time. The phase evolution of the Kuramoto modes instead is

$$\dot{\psi}_i=-\tilde{\delta}-\frac{\tilde{g}}{\mathcal{N}}\sum_{\substack{j=1\\ j\neq i}}^{\mathcal{N}}\cos(\tilde{\Theta}+\psi_j-\psi_i)\frac{\rho_j}{\rho_i}-\frac{\tilde{\eta}}{\rho_i}\sin(\Theta_D-\psi_i), \qquad (12)$$

with the renormalized driving strength $\tilde{\eta}$ and phase delay Θ_D given by

$$\tilde{\eta}e^{i\Theta_D}=\eta\frac{ge^{i\Theta}}{\frac{\Delta\omega-i\Delta\gamma}{2}\pm\mu}. \qquad (13)$$

In the long-time limit the ratios ρ_j/ρ_i approach unity, in which case Eq. (12) resembles a class of all-to-all coupled Kuramoto model [5]. This is illustrated in Fig. 3(b), and the consequence can be seen in Fig. 3(c) as all phases collapse to the same value. For times longer than this decoupling time, we can approximately find solutions for synchronization within the reduced Kuramoto basis.

For $\eta=0$, the complex amplitudes approach the same value if the isolated eigenmode is decaying faster than the other eigenmodes since then the transformation $\mathcal{U}$ mixes the long-living eigenmode at equal weight into all π_i. For $\eta>0$, the amplitudes ρ_i reach the same steady state since the effective driving as well as the decay rates are identical in the collective basis; an approximate mapping onto Sakaguchi-Kuramoto model with driving and all-to-all coupling is obtained. Due to the frequency distribution of the form $\delta(\omega-\omega_{\text{eff}})$, the system can synchronize for any coupling strength $\tilde{g}>0$ independent of $\tilde{\Theta}$ and η [8,10]. Therefore, all Kuramoto modes are synchronized, except for π_0. In the undriven case, the phases of the Kuramoto modes and the eigenmode are unrelated, and synchronization of the modes $\alpha_1,\dots,\alpha_\mathcal{N}$ in the bare basis is achieved since the back transformation $\mathcal{U}^{-1}$ treats these modes identically. Full synchronization, meaning that also the auxiliary mode α_0 attains the same phase as the other modes, is obtained if additionally the condition

$$\tan\Theta=-\frac{\gamma-\gamma_0}{\omega-\omega_0}=-\frac{\Delta\gamma}{\Delta\omega} \qquad (14)$$

is obtained, thus identical to Eq. (5) obtained in the full model. For $\eta>0$, the phases of all oscillators in the Kuramoto basis are equal for $t>\tau_{\text{sync}}$, and synchronization of all modes in the bare bases leads to

$$\tan\Theta=-\frac{\gamma}{\omega-\Omega}, \qquad (15)$$

which is the same condition for synchronization as in (6).

For both the driven and the undriven cases, the mechanism of synchronization of the main modes can therefore be led back to derivations of Kuramoto models which are exactly solvable. If additionally the conditions (5) (for undriven case) or (6) (for the driven case) are fulfilled, all phases including that of the auxiliary mode approach the same steady-state phase consistent with results previously highlighted.

V. DISCUSSION

Two fundamental aspects can strongly perturb synchronization: the effect of external noise and the inherent frequency disorder in the system. To model external noise we consider a thermal bath where a random stochastic force is responsible both for the decay of amplitudes as well as for the thermalization to the temperature of the environment. To incorporate effects stemming from disorder, we will consider variations in the oscillator frequencies according to a Gaussian distribution of increasing variance and with average ω.

A. Thermal noise

We consider the stochastic equations of motion for the complex amplitudes α_i in the presence of thermal noise

$$d\mathbf{A} = (-i\mathcal{H}\mathbf{A} + \eta\mathbf{u})dt + id\mathbf{W}, \tag{16}$$

where $d\mathbf{W} = (dW_0, dW_1, \ldots, dW_{\mathcal{N}})^T$ denotes a vector of $\mathcal{N}+1$ zero-averaged independent Wiener increments with $\langle dW_i\rangle = 0$ and correlations $\langle dW_i dW_j\rangle = \delta_{i,j}\,\xi_i\xi_j dt$ (see Appendix D). The noise entering the system comes from a bath at temperature T, which enters in the weights $\xi_i = \sqrt{2\gamma_i n_i(T)}$ depending on the loss rates $\gamma_{i=0} = \gamma_0, \gamma_{i>0} = \gamma$, and the average occupation number $n_i = k_B T/\hbar\omega_i$, with the frequencies $\omega_{i=0} = 0, \omega_{i>0} = \omega$. We solve Eq. (16) numerically by drawing random sample paths. To test the resilience against thermal noise we follow the time evolution of the variance of the phase.

In the undriven case $\eta = 0$, synchronization is preserved as long as the amplitude of each oscillator is larger than the fluctuations. The system is then synchronized only for $\tau_{\text{sync}} < t < \tau_{\text{noise}}$, where τ_{noise} denotes the time by which the system is dominated by thermal noise. Numerical results [see Fig. 4(a)] show that the variance of the mean phase diverges for $t \to \infty$. For $\eta > 0$, the system always remains synchronized as the variance is bounded. Therefore the phase difference with respect to the auxiliary mode cannot grow arbitrarily large and stays close to the average value [see Fig. 4(a)]. By incorporating only thermal noise, we restricted ourselves to the classical limit, albeit the non-Hermitian Hamiltonian formalism permits a genuine quantum treatment. The question how quantum effects affect synchronization is yet to clarify and requires an equation of motion adapted specifically to quantum noise.

B. Frequency disorder

In order to tackle the question of disorder, we allow the frequencies of the main modes to be disordered with a distribution $g(\omega)$ peaked around the mean frequency $\bar{\omega}$. For $g(\omega) = \exp[-(\omega-\bar{\omega})^2/2\sigma^2]$ the synchronization conditions hold for small $\sigma \ll \bar{\omega}$, but the steady state $\Delta\phi = \phi_0 - \phi_i$ is distributed normally with a modified variance σ_ϕ depending on the interaction strength, the width σ, and Θ [see Fig. 4(b)]. Interestingly, σ_ϕ is proportional to σ, i.e., $\sigma_\phi = c(g,\Theta)\sigma$ and $c(g,\Theta)$ is largest at $\Theta = \pi/2$. For arbitrarily large σ, however, the distribution becomes more complex, and in the limit $\sigma \gg \bar{\omega}$ a chimera-like distribution is approached, where the population of oscillators is split into two groups. For $\Theta = \pi/2$, the distribution is symmetric around $\Delta\phi = 0$ with the two peaks at $\pm\pi/2$. Since the peaks become the narrower the larger σ is, the phase coherence z can be used to distinguish different regimes. Weak disorder leads to a nearly synchronized population, and thus $z \approx 1$. The more the distribution separates into two subgroups, the smaller is z, which converges to 0 algebraically. In principle, one could again apply the formalism presented in the last section using a transformation into the Kuramoto basis. However, due to nonuniform frequencies, not only are the eigenmode and the Kuramoto mode coupled, but also the all-to-all coupling now has a random strength which complicates analytical considerations drastically. Therefore, the complete investigation of this question needs further research.

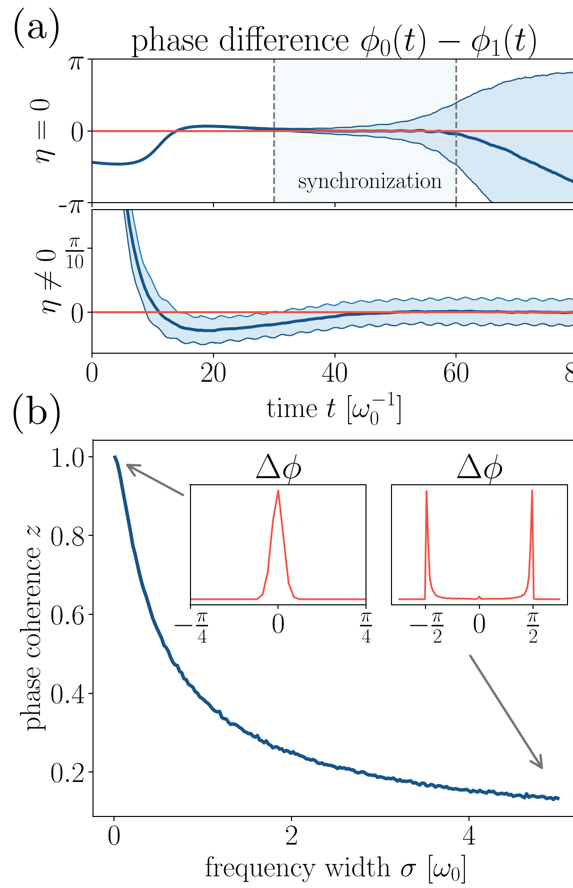

FIG. 4. (a) Phase difference between two coupled oscillators with additional noise. In the undriven case with $\eta = 0$ and $\Theta = 3\pi/4$ the oscillators synchronize, but the variance increases linearly at some time and the mean value deviates from zero. For the driven system with $\eta = 1$ and $\Theta = \pi/2$, the variance and mean value remain finite and zero, respectively. (b) Phase coherence as a function of the frequency disorder σ. For small σ the distribution is approximately Gaussian, and thus $z \approx 1$. For $\Theta = \pi/2$, the distribution approaches a balanced bimodal distribution where the peaks are located at $\pm\pi/2$. Therefore $z \to 0$ for $\sigma \to \infty$ since the width of both peaks decreases with increasing disorder. Parameters are $\omega_0 = 1.0$, $\omega = 1.1$, $\gamma_0 = 0.1$, $\gamma = 0.2$, $g = 0.1$, $\Omega = 1.1$, and $\eta = 1.0$.

VI. CONCLUSIONS

We have studied the interplay between non-Hermitian couplings and phase synchronization, at the classical level, in a system of $\mathcal{N}+1$ bosonic modes. We show the emergence of regimes of phase synchronization which, owing to the linearity of the evolution matrix, can be fully analytically tackled. We find that the crucial parameter connected to synchronization is the non-Hermitian coupling strength. In order to better understand the occurrence of phase synchronization in a linearly evolving system, we show that a mapping onto a nonlinear reduced model of $\mathcal{N}$ collective modes shows an intrinsic connection to the standard Kuramoto nonlinear model. Future investigations will see the extension of our model to the question of quantum synchronization. Such effects could be experimentally tested on a variety of platforms where non-Hermitian dynamics can be generated via the elimination of lossy, auxiliary modes. Among these, one can envision testing of phase synchronization in optomechanical or optomagnonical systems or in the context of cavity quantum electrodynamics with molecules, where additionally the effect of collective mode pulling or mode attraction via the common coupling to a cavity-quantized mode could be tackled.

ACKNOWLEDGMENTS

We acknowledge useful discussions with Muhammad Asjad and Christian Sommer. We acknowledge financial support from the Max Planck Society and from the Deutsche Forschungsgemeinschaft (DFG, German Research Foundation), Project-ID 429529648, TRR 306 QuCoLiMa ("Quantum Cooperativity of Light and Matter").

APPENDIX A: KURAMOTO MODEL

A simple model that demonstrates synchronization is the Kuramoto model. Denoting the phases of $\mathcal{N}$ oscillators with ϕ_i, their equations of motion are given by

$$\dot{\phi}_i = \omega_i + \frac{K}{\mathcal{N}} \sum_{j=1}^{\mathcal{N}} \sin(\phi_j - \phi_i). \tag{A1}$$

Here ω_i is the natural frequency of the i-th oscillator meaning its frequency in the case of free evolution. Provided the strength K is sufficiently large, the nonlinear, all-to-all coupling then forces more and more oscillators to assume an entrained frequency as well as their phases to be close. Thus, the model features synchronization. In order to define a quantity representing the quality of synchronization, the phase coherence z

$$z := \left| \frac{1}{\mathcal{N}} \sum_{i=1}^{\mathcal{N}} e^{i\phi_i} \right| \tag{A2}$$

is introduced. If all phases are uniformly distributed, one obtains $z = 0$, and the system is found to be in an absolute nonsynchronized state. In contrast, $z = 1$ represents the perfectly synchronized case where all phases equal each other. In the limit $\mathcal{N} \to \infty$, a self-consistency ansatz permits one to analytically determine how the distribution $g(\omega)$ of natural frequencies ω_i and coupling strength K affects the steady-state value of z. For example, for a Lorentzian distribution of width Δ and mean frequency ω, it turns out that synchronization is achieved only if K exceeds a critical value given by $K_{\text{crit}} = 2\Delta$. Below this threshold, the system always remains in an unsynchronized state ($z = 0$), whereas above it approaches the perfectly synchronized state ($z = 1$) as K grows. The phase coherence $z = 1$ can be seen as an order parameter that distinguishes an unsynchronized and a synchronized phase, separated by a second-order-like phase transition.

The Kuramoto model can be naturally extended, for example, by modifying the interaction term or adding a driving term. In a frame, rotating at frequency Ω of the driving, the equations of motion, that are particularly interesting for the considerations in this paper, read

$$\dot{\phi}_i = \omega_i + \frac{K}{\mathcal{N}} \sum_{i=1}^{\mathcal{N}} \sin(\phi_j - \phi_i + \alpha) - \eta \sin \phi_i. \tag{A3}$$

Without the driving term ($\eta = 0$), the model above is known as Sakaguchi-Kuramoto model, which adds a phase shift α to the nonlinear interaction term. If all oscillators have the same natural frequency $\omega_i = \omega$, the system always synchronizes.

APPENDIX B: NON-HERMITIAN DYNAMICS

Let us first justify how an effective non-Hermitian interaction can occur via elimination of an auxiliary, lossy degree of freedom and then move on to write the equations of motion for the complex amplitudes and real amplitudes and phases.

1. Effective non-Hermitian interactions

Let us consider the Hamiltonian for three modes

$$H_0 = \omega_1 a_1^\dagger a_1 + \omega_2 a_2^\dagger a_2 + \Omega \Lambda^\dagger \Lambda + (g_1 a_1^\dagger + g_2 a_2^\dagger)\Lambda + \text{H.c.}, \tag{B1}$$

where $\omega_1, \omega_2, \Omega$ denote the frequencies modes a_1, a_2 and the auxiliary mode Λ. The coupling strengths g_1, g_2 are allowed to be complex, but the total interaction term is still defined to be Hermitian. Explicitly writing out the equations of motion for the expectation values $\alpha_i := \langle a_i \rangle$ and $\lambda := \langle \Lambda \rangle$ yields

$$\begin{aligned} \dot{\alpha}_i(t) &= -i(\omega_i - i\gamma_i)\alpha_i(t) - ig_i\lambda(t), \\ \dot{\lambda}(t) &= -i(\Omega - i\Gamma)\lambda(t) - i[g_1^*\alpha_1(t) + g_2^*\alpha_2(t)]. \end{aligned} \tag{B2}$$

where $\gamma_1, \gamma_2, \Gamma$ are the loss rates which are included as usual in Lindblad form in the master equation. Formally integrating the second equation then leads to

$$\lambda(t) = e^{-i(\Omega - i\Gamma)t}\lambda(0) - i\int_0^t dt'[g_1^*\alpha_1(t') + g_2^*\alpha_2(t')] \times e^{-i(\Omega - i\Gamma)(t-t')}. \tag{B3}$$

We now focus on the case $\Gamma \gg \Omega, \omega_i, \gamma_i, g_i$ and try to approximate the integral in the equation above. Therefore, terms like $\int_0^t dt' g_i^* \alpha_i(t') e^{-i(\Omega - i\Gamma)(t-t')}$ are integrated by parts and terms where fractions of ω_i, γ_i or g_i over Γ occur are neglected. The simplified expression for $\lambda(t)$ can then be inserted into the equations for $\dot{\alpha}_i$ in Eq. (B2) resulting in two equations which are completely decoupled from the auxiliary mode

$$\begin{aligned}\dot{\alpha}_i &= -i(\omega_i - i\gamma_i)\alpha_i - ig_i\left(e^{-i(\Omega-i\Gamma)t}\lambda(0) - \frac{1}{\Omega-i\Gamma}[g_1^*\alpha_1(t) - \alpha_1(0)e^{-i(\Omega-i\Gamma)t}] + g_2^*[\alpha_2(t) - \alpha_2(0)e^{-i(\Omega-i\Gamma)t}]\right)\\ &\approx -i\left(\left(\omega_i - \frac{|g_i|^2\Omega}{\Omega^2+\Gamma^2}\right) - i\left(\gamma_i + \frac{|g_i|^2\Gamma}{\Omega^2+\Gamma^2}\right)\right)\alpha_i + ig_i\frac{\Omega+i\Gamma}{\Omega^2+\Gamma^2}g_{i-1}^*\alpha_{i-1}.\end{aligned} \tag{B4}$$

Thus, the same dynamics of the complex amplitudes α_i is obtained by considering the effective Hamiltonian

$$H_{\mathrm{NH}}^{\mathrm{eff}} = \omega_1^{\mathrm{eff}}a_1^\dagger a_1 + \omega_2^{\mathrm{eff}}a_2^\dagger a_2 + g_{1,2}^{\mathrm{eff}}a_1^\dagger a_2 + g_{2,1}^{\mathrm{eff}}a_2^\dagger a_1 \tag{B5}$$

with non-Hermitian coupling strengths

$$g_{i,i+1}^{\mathrm{eff}} = -g_i\frac{\Omega+i\Gamma}{\Omega^2+\Gamma^2}g_{i+1}^* \approx -i\frac{g_ig_{i+1}^*}{\Gamma} \tag{B6}$$

and renormalized frequencies and coupling strengths

$$\begin{aligned}\omega_i^{\mathrm{eff}} &= \omega_i - \frac{|g_i|^2\Omega}{\Omega^2+\Gamma^2} \approx \omega_i,\\ \gamma_i^{\mathrm{eff}} &= \gamma_i + \frac{|g_i|^2\Gamma}{\Omega^2+\Gamma^2} \approx \gamma_i + \frac{|g_i|^2}{\Gamma}.\end{aligned} \tag{B7}$$

Notice that in addition to the effective couplings, the bare frequencies and damping rates are also changed. We can check the accuracy of this adiabatic elimination by comparing the spectra of H_0 and $H_{\mathrm{NH}}^{\mathrm{eff}}$ as a function of the frequency detuning $\delta = \omega_1 - \omega_2$ for the sample values $\omega_1 = 1.0 + \delta$, $\omega_2 = \Omega = 1.0$, $\gamma_1 = 0.01$, $\gamma_2 = 0.012$, $\Gamma = 10.0$ and $g_1 = g_2 = 0.5$. As shown in Fig. 5, the approximation works quite well independently of δ. Therefore, non-Hermitian interactions can be used to effectively describe two modes which are indirectly coupled via a lossy auxiliary mode.

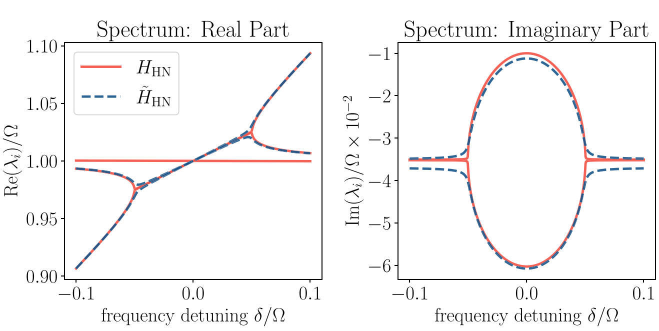

FIG. 5. Real part and imaginary part of the eigenvalues λ_i of both the exact as well as of the effective (reduced) Hamiltonians as a function of the frequency detuning $\delta = \omega_1 - \omega_2$ for the sample values $\omega_1 = 1.0 + \delta$, $\omega_2 = \Omega = 1.0$, $\gamma_1 = 0.01$, $\gamma_2 = 0.012$, $\Gamma = 10.0$, and $g_1 = g_2 = 0.5$.

2. Equations of motion for amplitudes and phases

Starting from the master equation, the dynamics of the expectation values $\alpha_i = \langle a_i\rangle$ in the corotating frame is

$$\begin{aligned}\dot{\alpha}_0 &= -i(\omega_0 - \Omega - i\gamma_0)\alpha_0 - i\frac{g}{\sqrt{\mathcal{N}}}e^{i\Theta}\sum_{j=1}^{\mathcal{N}}\alpha_j + \eta,\\ \dot{\alpha}_i &= -i(\omega - \Omega - i\gamma)\alpha_i - i\frac{g}{\sqrt{\mathcal{N}}}e^{i\Theta}\alpha_0,\end{aligned} \tag{B8}$$

thus, leading to the matrix-vector form

$$\dot{\mathbf{A}} = -i\mathcal{H}\mathbf{A} + \eta(1, 0, \ldots)^T \tag{B9}$$

with $\mathbf{A} = (\alpha_0, \alpha_1, \ldots, \alpha_{\mathcal{N}})^T$ and

$$\mathcal{H} = \begin{pmatrix} \delta_0 - i\gamma_0 & \frac{g}{\sqrt{\mathcal{N}}}e^{i\Theta} & \cdots & \frac{g}{\sqrt{\mathcal{N}}}e^{i\Theta}\\ \frac{g}{\sqrt{\mathcal{N}}}e^{i\Theta} & \delta - i\gamma & & \\ \vdots & & \ddots & \\ \frac{g}{\sqrt{\mathcal{N}}}e^{i\Theta} & & & \delta - i\gamma \end{pmatrix}, \tag{B10}$$

where $\delta_{(0)} = \omega_{(0)} - \Omega$ (for the case $\eta = 0$, set $\Omega = 0$, so that $\delta = \omega$). This set of $\mathcal{N} + 1$ linear, complex-valued equations can be brought into a system of $2(\mathcal{N} + 1)$, nonlinear equations by separating the complex amplitudes α_i into real-value amplitudes and phases, i.e., $\alpha_i = r_ie^{i\phi_i}$ with $r_i \equiv |\alpha_i|$, $\phi_i \equiv \arg\alpha_i$. The derivative on the left side of Eq. (B9) reads $\dot{\alpha}_i = \dot{r}_ie^{i\phi_i} + i\dot{\phi}_i r_ie^{i\phi_i}$ so that by replacing α_i by $r_ie^{i\phi_i}$ both sides can be decomposed into real and imaginary parts. When separating the equations and moving the exponential to the right hand side, the driving of the auxiliary mode separates into a cosine and a sine. This yields two sets of coupled equations, $\mathcal{N} + 1$ equations determining the evolution of the real-valued amplitudes

$$\begin{aligned}\dot{r}_0 &= -\gamma_0r_0 + \frac{g}{\sqrt{\mathcal{N}}}\sum_{j=1}^{\mathcal{N}}\sin(\Theta + \phi_j - \phi_0)r_j + \eta\cos\phi_0,\\ \dot{r}_i &= -\gamma r_i + \frac{g}{\sqrt{\mathcal{N}}}\sin(\Theta + \phi_0 - \phi_i)r_0, \quad i = 1, \ldots, \mathcal{N}\end{aligned} \tag{B11}$$

and $\mathcal{N} + 1$ equations for the phases

$$\begin{aligned}\dot{\phi}_0 &= -\delta_0 - \frac{g}{\sqrt{\mathcal{N}}}\sum_{j=1}^{\mathcal{N}}\frac{r_j}{r_0}\cos(\Theta + \phi_j - \phi_0) - \eta\sin\phi_0,\\ \dot{\phi}_i &= -\delta - \frac{g}{\sqrt{\mathcal{N}}}\frac{r_0}{r_i}\cos(\Theta + \phi_0 - \phi_i), \quad i = 1, \ldots, \mathcal{N}.\end{aligned} \tag{B12}$$

Apparently, we obtain a Kuramoto-like interaction for $\Theta = \pi/2$. If we assume that the ratio r_i/r_j is nearly constant after a sufficiently long settling time (as apparent from numerical simulations), the equation for the phases decouples from the amplitude equations and a Kuramoto model with a $\mathcal{N}$-to-1 coupling is effectively obtained. Since there is an analytical solution for the Kuramoto model with an all-to-all coupling in the limit $\mathcal{N} \to \infty$, we present next a basis transformation that introduces all-to-all coupled, collective modes thus leading to the original Kuramoto model.

APPENDIX C: PHASE SYNCHRONIZATION

1. Mapping onto the Kuramoto model

In order to map the non-Hermitian synchronization model onto an analytically solvable all-to-all coupled Kuramoto model, we first diagonalize the evolution matrix $\mathcal{H}$ and then find a transformation which turns $\mathcal{H}$ into another matrix $\mathcal{M}$ which possesses entries coupling $\mathcal{N}$ of the total $\mathcal{N}+1$ modes to $\mathcal{N}$ modes with equal strength. The remaining mode is an eigenmode which does not interact with any other mode.

Note that as $\mathcal{H}$ is non-Hermitian, there are sets of parameters $\delta_{(0)}, \gamma_{(0)}, g, \Theta$ which lead to a nondiagonalizable matrix. Nevertheless, one can show that in most cases we can simply assume that $\mathcal{H}$ is similar to a diagonal matrix $\mathcal{D}$. The Fourier transformation $\mathcal{T}$ acting only on the $\mathcal{N}\times\mathcal{N}$ subspace of nonauxiliary modes

$$\mathcal{T} = \begin{pmatrix} 1 & 0 \\ 0 & \mathcal{F} \end{pmatrix}, \qquad \mathcal{F}_{i,j} = \frac{1}{\sqrt{\mathcal{N}}} e^{i\frac{2\pi ij}{\mathcal{N}}}, \quad i, j = 1, \dots, \mathcal{N} \tag{C1}$$

introduces from a physical point of view a so-called bright mode interacting with the auxiliary mode while $\mathcal{N}-1$ dark modes do not participate in system and remain isolated. More precisely, the matrix $\mathcal{T}\mathcal{H}\mathcal{T}^{-1}$ reduces the task to an effective 2×2 diagonalization problem. One can show that by the transformation $\mathcal{S}_\pm$,

$$\mathcal{S}_\pm = \begin{pmatrix} 1 & 0 & \dots & 0 & s_\pm \\ 0 & & & & 0 \\ \vdots & & \mathbb{1}_{\mathcal{N}-1} & & \vdots \\ 0 & & & & 0 \\ -s_\pm & 0 & \dots & 0 & 1 \end{pmatrix},$$

$$s_\pm = \frac{g e^{i\Theta}}{\frac{\Delta\omega - i\Delta\gamma}{2} \pm \mu} = -\frac{\frac{\Delta\omega - i\Delta\gamma}{2} \mp \mu}{g e^{i\Theta}}, \tag{C2}$$

with $\Delta\omega = \omega_0 - \omega$, $\Delta\gamma = \gamma_0 - \gamma$ and $\mu = \sqrt{(\frac{\Delta\omega - i\Delta\gamma}{2})^2 + g^2 e^{2i\Theta}}$ the final step towards the diagonal matrix $\mathcal{D}_\pm$ is accomplished. The sign $\pm$ denotes only the order of eigenvalues on the diagonal. In fact, one finds three different eigenvalues, thus obtaining

$$\mathcal{D}_\pm = (\mathcal{S}_\pm\mathcal{T})\mathcal{H}(\mathcal{S}_\pm\mathcal{T})^{-1} = \begin{pmatrix} \frac{\Delta\omega - i\Delta\gamma}{2} \pm \mu & & & & \\ & 0 & & & \\ & & \ddots & & \\ & & & 0 & \\ & & & & \frac{\Delta\omega - i\Delta\gamma}{2} \mp \mu \end{pmatrix} + (\delta - i\gamma)\mathbb{1}_{\mathcal{N}+1}. \tag{C3}$$

It is now straightforward to see that

$$\mathcal{V} = \begin{pmatrix} 1 & 0 & \dots & 0 & 0 \\ 0 & & & & 1 \\ \vdots & & -\mathbb{1}_{\mathcal{N}-1} & & \vdots \\ 0 & & & & 1 \\ 0 & 1 & \dots & 1 & 1 \end{pmatrix} \tag{C4}$$

yields the basis transformation we searched for, since

$$\mathcal{M}_\pm = (\mathcal{V}\mathcal{S}_\pm\mathcal{T})\mathcal{H}(\mathcal{V}\mathcal{S}_\pm\mathcal{T})^{-1} = \begin{pmatrix} \frac{\Delta\omega - i\Delta\gamma}{2} \pm \mu & 0 & \dots & 0 \\ 0 & \frac{\Delta\omega - i\Delta\gamma \mp 2\mu}{2\mathcal{N}} & \dots & \frac{\Delta\omega - i\Delta\gamma \mp 2\mu}{2\mathcal{N}} \\ \vdots & \vdots & & \vdots \\ 0 & \frac{\Delta\omega - i\Delta\gamma \mp 2\mu}{2\mathcal{N}} & \dots & \frac{\Delta\omega - i\Delta\gamma \mp 2\mu}{2\mathcal{N}} \end{pmatrix} + (\delta - i\gamma)\mathbb{1}_{\mathcal{N}+1}. \tag{C5}$$

The choice between the M_+ or M_- version enables us to select one of the eigenvalues to be isolated, whereas the remaining ones are mixed in the lower left block thereby introducing all-to-all couplings of equal strength scaling with $\mathcal{N}^{-1}$.

We can now transform Eq. (B9) into the collective basis, which we will also refer to as the Kuramoto basis. With $\mathbf{P} = \mathcal{V}\mathcal{S}\mathcal{T}\mathbf{A} = (\pi_0, \pi_1, \dots, \pi_\mathcal{N})^T$, the equation of motion in the new basis is given by $\dot{\mathbf{P}} = -i\mathcal{M}\mathbf{P} + \eta\mathcal{V}\mathcal{S}\mathcal{T}(1, 0, \dots)^T$. In a componentwise notation, the equations read

$$\dot{\pi}_0 = -i\big(\delta_0^{\text{eff}} - i\gamma_0^{\text{eff}}\big)\pi_0 + \eta,$$
$$\dot{\pi}_i = -i(\delta^{\text{eff}} - i\gamma^{\text{eff}})\pi_i - i\frac{K_{\text{eff}} e^{i\Theta_{\text{eff}}}}{\mathcal{N}} \sum_{j\neq i}^{\mathcal{N}} \pi_j - \eta_{\text{eff}} e^{i\Theta_{\text{drive}}} \tag{C6}$$

with effective frequencies

$$\delta_0^{\rm eff} - i\gamma_0^{\rm eff} = \delta - i\gamma + \frac{\Delta\omega - i\Delta\gamma \pm 2\mu}{2},$$
$$\delta^{\rm eff} - i\gamma^{\rm eff} = \delta - i\gamma + \frac{\Delta\omega - i\Delta\gamma \mp 2\mu}{2\mathcal{N}} \tag{C7}$$

and coupling parameters

$$K_{\rm eff}e^{i\Theta_{\rm eff}} = \tfrac{1}{2}(\Delta\omega - i\Delta\gamma \mp 2\mu). \tag{C8}$$

Due to a complex prefactor in the transformation, the modes with $i = 1, \ldots, \mathcal{N}$ are driven with strength $\eta_{\rm eff}$ and a phase shift $\Theta_{\rm drive}$ whereby

$$\eta_{\rm eff} = |s_\pm|\eta,$$
$$\Theta_{\rm drive} = \arg s_\pm. \tag{C9}$$

Finally, the separation into equations for phases $\psi_i := \arg\pi_i - \Theta_{\rm drive}$ and real amplitudes $\rho_i := |\pi_i|$ for the coupled modes leads to

$$\dot\rho_i = -\gamma_{\rm eff}\rho_i + \frac{K_{\rm eff}}{\mathcal{N}}\sum_{j\neq i}^{\mathcal{N}}\rho_j \sin(\Theta_{\rm eff} + \psi_j - \psi_i) + \eta_{\rm eff}\cos\psi_i,$$
$$\dot\psi_i = -\delta_{\rm eff} - \frac{K_{\rm eff}}{\mathcal{N}}\sum_{j\neq i}^{\mathcal{N}}\frac{\rho_j}{\rho_i}\cos(\Theta_{\rm eff} + \psi_j - \psi_i) - \frac{\eta_{\rm eff}}{\rho_i}\sin\psi_i,$$
$$i = 1, \ldots, \mathcal{N}. \tag{C10}$$

The phase equations decouple from the amplitude equations after a sufficiently long time, since, first, the long-term behavior is dominated by the driving, which pumps each collective mode equally (except for the eigenmode of course). Second, a steady state is reached where $\rho_i = \rho =$ const, thus ensuring that the two equations decouple. Also in the undriven case $\eta = 0$, the ratios $\rho_i/\rho_j \to 1$, since all collective modes are linear combinations of the eigenmodes given by $\mathcal{V}$. A look at the diagonal matrix in Eq. (C3) only one eigenmode survives in the long-time limit, corresponding to either the eigenvalue $(\Delta\omega - i\Delta\gamma)/2 + \mu$ or $(\Delta\omega - i\Delta\gamma)/2 - \mu$. By choosing one of the transformations $\mathcal{S}_\pm$, we always can choose the fast decaying eigenmode to be the isolated mode in the new Kuramoto basis. Then for initial complex amplitudes $\mathbf{A} = (\alpha_0(0), \alpha_1(0), \ldots)^T$ and a short notation for the eigenvalues $\lambda_0 = (\Delta\omega - i\Delta\gamma)/2 \pm \mu$, $\lambda_{0<j<\mathcal{N}} = \omega - i\gamma$, $\lambda_{\mathcal{N}} = (\Delta\omega - i\Delta\gamma)/2 \mp \mu$ one obtains

$$\frac{\pi_i}{\pi_j} = \frac{\sum_k \mathcal{V}_{i,k}e^{-i\lambda_k t}[\mathcal{S}_\pm\mathcal{T}\mathbf{A}(0)]_k}{\sum_k \mathcal{V}_{j,k}e^{-i\lambda_k t}[\mathcal{S}_\pm\mathcal{T}\mathbf{A}(0)]_k}$$
$$\to \frac{\mathcal{V}_{i,\mathcal{N}}e^{-i\lambda_{\mathcal{N}} t}[\mathcal{S}_\pm\mathcal{T}\mathbf{A}(0)]_{\mathcal{N}}}{\mathcal{V}_{j,\mathcal{N}}e^{-i\lambda_{\mathcal{N}} t}[\mathcal{S}_\pm\mathcal{T}\mathbf{A}(0)]_{\mathcal{N}}} = 1,$$
$$i, j = 1, \ldots, \mathcal{N}. \tag{C11}$$

We can therefore set $\rho_i/\rho_j \approx 1$ and concentrate on the phase equations which now clearly represent variations of the Kuramoto model with all-to-all couplings. In particular, for $\Theta_{\rm eff} = \pi/2$, the phases ψ_i evolve according to

$$\dot\psi_i = -\delta_{\rm eff} + \frac{K_{\rm eff}}{\mathcal{N}}\sum_{j\neq i}^{\mathcal{N}}\sin(\psi_j - \psi_i) - \frac{\eta_{\rm eff}}{\rho}\sin\psi_i, \tag{C12}$$

which is the *Kuramoto model* [5] with driving. In conclusion, the non-Hermitian dynamics can be mapped onto variations of the Kuramoto model with all-to-all coupling.

2. Synchronization in the Kuramoto basis

We showed, that in the long-time limit the phase equations for the Kuramoto modes are given by

$$\dot\psi_i = -\delta_{\rm eff} - \frac{K_{\rm eff}}{\mathcal{N}}\sum_{j\neq i}^{\mathcal{N}}\cos(\Theta_{\rm eff} + \psi_j - \psi_i) - \frac{\eta_{\rm eff}}{\rho}\sin\psi_i. \tag{C13}$$

We can now investigate synchronization behavior of this reduced model by taking advantage of existing solutions. We first start with the undriven case $\eta = 0$ and assume large $\mathcal{N}$ since many exact results we cite rely on this requirement. However, the key message also holds for small $\mathcal{N}$.

In case of $\eta = 0$, Eq. (C13) is known as the *Sakaguchi-Kuramoto model* for which an analytical solution is provided. In the case of a frequency distribution $g(\omega) = \delta(\omega - \omega_{\rm eff})$, synchronization is expected to occur for any $K_{\rm eff} > 0$. More importantly, in the final, stationary state all phases ψ_i are equal, i.e., the synchronization order parameter z defined by $ze^{i\Psi} := \sum_i e^{i\psi_i}$ is $z = 1$. Consequently, the mean frequency is $\bar\omega = -\omega_{\rm eff} - K_{\rm eff}\cos\Theta_{\rm eff}$.

Apparently, in the Kuramoto basis all coupled modes synchronize while the remaining eigenmode decays significantly faster, and therefore the amplitude vector is approximately

$$\mathbf{P}(t) \to \begin{pmatrix} 0 \\ \rho e^{i\Psi(t)} \\ \vdots \\ \rho e^{i\Psi(t)} \end{pmatrix}. \tag{C14}$$

If the back transformation $\mathbf{A} = (\mathcal{V}\mathcal{S}_\pm\mathcal{T})^{-1}\mathbf{P}(t)$ is supposed to protect the synchronization behavior, the phase of all α_i must be the same. The special property of $(\mathcal{V}\mathcal{S}_\pm\mathcal{T})^{-1}$,

$$(\mathcal{V}\mathcal{S}_\pm\mathcal{T})^{-1}\begin{pmatrix} 0 \\ 1 \\ \vdots \\ 1 \end{pmatrix} \propto \begin{pmatrix} -\sqrt{\mathcal{N}}s_\pm \\ 1 \\ \vdots \\ 1 \end{pmatrix}, \tag{C15}$$

then leads to synchronization conditions, since $s_\pm$ must be real. Otherwise the phase of the auxiliary mode α_0 would be different from the other phases. One can show that $s_\pm \in \mathbb{R}$ is satisfied if

$$\tan\Theta = -\frac{\Delta\gamma}{\Delta\omega}, \tag{C16}$$

which is differently derived in the subsequent section. To further rule out the case of a phase shift of π between the auxiliary mode and the main modes, $s_\pm < 0$ is required, which leads to the additional condition $\Delta\gamma\sin\Theta < \Delta\omega\cos\Theta$.

The synchronization conditions can be derived in a similar way for the driven case $\eta \neq 0$. Equation (C13) is solved for $\psi_i = \psi_j \equiv \psi$ and a steady-state amplitude $\rho_i = \rho$ given by

$$\rho e^{i\psi} = \frac{is_+\eta}{\delta - i\gamma + \frac{\Delta\omega - i\Delta\gamma - 2\mu}{2}}, \tag{C17}$$

where the $+$-version of the transformation $(\mathcal{V}\mathcal{S}_\pm\mathcal{T})$ was chosen. The steady state of the isolated mode is

$$\rho_0 e^{i\psi_0} = -\frac{i\eta}{\delta - i\gamma + \frac{\Delta\omega - i\Delta\gamma + 2\mu}{2}}, \tag{C18}$$

and by performing the back transformation $\mathbf{A} = (\mathcal{V}\mathcal{S}_+\mathcal{T})^{-1}\mathbf{P}$ again, one finds that the phases remain synchronized in the bare basis only if the synchronization conditions

$$\tan\Theta = -\frac{\gamma}{\omega - \Omega}, \quad (\omega - \Omega)\cos\Theta < \gamma\sin\Theta \tag{C19}$$

are satisfied. In fact, these conditions ensure that the relative phases of the modes are unaffected by the transformation $\mathcal{V}\mathcal{S}_+\mathcal{T}$.

3. Derivation of synchronization conditions for non-Hermitianly coupled modes

The system is synchronized if $\mathrm{Im}(\alpha_j/\alpha_0)|_{t\to\infty} = 0$ and $\mathrm{Re}(\alpha_j/\alpha_0)|_{t\to\infty} > 0$ since then $\phi_j = \phi_0$ for $t \to \infty$. To calculate those ratios of complex amplitudes, Eq. (B9) is solved by diagonalizing $\mathcal{H} = (\mathcal{S}_\pm\mathcal{T})^{-1}\mathcal{D}_\pm(\mathcal{S}_\pm\mathcal{T})$,

$$\mathbf{A}(t) = (\mathcal{S}_\pm\mathcal{T})^{-1}e^{-i\mathcal{D}_\pm(t-t_0)}(\mathcal{S}_\pm\mathcal{T})\mathbf{A}(t_0) + \eta\int_{t_0}^{t} dt'(\mathcal{S}_\pm\mathcal{T})^{-1}e^{-i\mathcal{D}_\pm(t-t')}(\mathcal{S}_\pm\mathcal{T})\begin{pmatrix}1\\0\\\vdots\\0\end{pmatrix}, \tag{C20}$$

with $t_0 = 0$.

We start with the case $\eta = 0$. In order to find α_i, α_0 the matrix-vector products in Eq. (C20) are carried out leading to

$$\alpha_j(t) = e^{-i(\omega - i\gamma)t}\sum_{l=0}^{\mathcal{N}}\alpha_l(0)\Bigg[(\mathcal{S}_\pm\mathcal{T})^{-1}_{j,0}(\mathcal{S}_\pm\mathcal{T})_{0,l}e^{-i(\frac{\Delta\omega - i\Delta\gamma}{2}\pm\mu)t} + \sum_{k=0}^{\mathcal{N}-1}(\mathcal{S}_\pm\mathcal{T})^{-1}_{j,k}(\mathcal{S}_\pm\mathcal{T})_{k,l} + (\mathcal{S}_\pm\mathcal{T})^{-1}_{j,\mathcal{N}}(\mathcal{S}_\pm\mathcal{T})_{\mathcal{N},l}e^{-i(\frac{\Delta\omega - i\Delta\gamma}{2}\mp\mu)t}\Bigg]. \tag{C21}$$

Considering the infinite-time limit $t \to \infty$, the first two lines are neglected under the assumption that without loss of generality $(\mathcal{D}_\pm)_{\mathcal{N}\mathcal{N}} = \frac{\Delta\omega - i\Delta\gamma}{2} \mp \mu$ is the long-living eigenvalue with the smallest imaginary part. Therefore, for $t \to \infty$ the last term dominates the other ones, and we can approximately write

$$\frac{\alpha_j}{\alpha_0} \approx \frac{e^{-i(\omega - i\gamma)t}\sum_{l=0}^{\mathcal{N}}\alpha_l(0)(\mathcal{S}_\pm\mathcal{T})^{-1}_{j,\mathcal{N}}(\mathcal{S}_\pm\mathcal{T})_{\mathcal{N},l}e^{-i(\frac{\Delta\omega - i\Delta\gamma}{2}\mp\mu)t}}{e^{-i(\omega - i\gamma)t}\sum_{l=0}^{\mathcal{N}}\alpha_l(0)(\mathcal{S}_\pm\mathcal{T})^{-1}_{0,\mathcal{N}}(\mathcal{S}_\pm\mathcal{T})_{\mathcal{N},l}e^{-i(\frac{\Delta\omega - i\Delta\gamma}{2}\mp\mu)t}} = \frac{(\mathcal{S}_\pm\mathcal{T})^{-1}_{j,\mathcal{N}}}{(\mathcal{S}_\pm\mathcal{T})^{-1}_{0,\mathcal{N}}} = -\frac{1}{\sqrt{\mathcal{N}}s_\pm}. \tag{C22}$$

Taking the imaginary and real part as well as inserting the definition of $s_\pm$ then finally leads to the synchronization conditions for the undriven case

$$\tan\Theta = -\frac{\Delta\gamma}{\Delta\omega} \tag{C23}$$

and

$$\Delta\gamma\sin\Theta < \Delta\omega\cos\Theta. \tag{C24}$$

The derivation for finite $\eta \neq 0$ is in principle similar. In contrast to the previous case, the term surviving for $t \to \infty$ is the integral term in Eq. (C20) and one can write

$$\alpha_k(t\to\infty) = \int_0^t dt'\sum_{l=0}^{\mathcal{N}}(\mathcal{S}_\pm\mathcal{T})^{-1}_{k,l}e^{-i(\mathcal{D}_\pm)_{l,l}(t-t')}(\mathcal{S}_\pm\mathcal{T})_{l,0} \to i\sum_{l=0}^{\mathcal{N}}\frac{(\mathcal{S}_\pm\mathcal{T})^{-1}_{k,l}(\mathcal{S}_\pm\mathcal{T})_{l,0}}{(\mathcal{D}_\pm)_{l,l}}. \tag{C25}$$

By inserting the corresponding expressions for the matrix elements and some mathematical reordering of terms one eventually finds that the ratio of complex amplitudes approaches a constant value

$$\frac{\alpha_k}{\alpha_0} \to -\frac{1}{\sqrt{\mathcal{N}}}\frac{ge^{i\Theta}}{\delta - i\gamma}, \quad t\to\infty. \tag{C26}$$

By requiring the imaginary part of the expression above to be zero the synchronization conditions

$$\tan\Theta = -\frac{\gamma}{\omega - \Omega} \tag{C27}$$

and

$$\cos\Theta(\omega - \Omega) < \sin\Theta\gamma \tag{C28}$$

are obtained.

APPENDIX D: DYNAMICS IN THE PRESENCE OF EXTERNAL NOISE

In order to test the resilience of synchronized systems against noise, we consider the system now to be exposed to classical, thermal noise. To this end, the complex amplitudes α_i are separated into real parts q_i, p_i, $\alpha_i = q_i + ip_i$ resembling position and momentum coordinates. We can then write two equations of motion for q_i and p_i and include thermal forces modeled by a Wiener process which is added to the equation for p_i,

$$\begin{aligned}
dq_0 &= \left[\omega_0 p_0 - \gamma_0 p_0 + \frac{g}{\sqrt{\mathcal{N}}}\sum_{i=1}^{\mathcal{N}}(\cos\Theta\, p_i + \sin\Theta\, q_i)\right]dt,\\
dq_i &= \left[\omega p_i - \gamma q_i + \frac{g}{\sqrt{\mathcal{N}}}(\cos\Theta\, p_0 + \sin\Theta\, q_0)\right]dt,\\
dp_0 &= \left[-\omega_0 q_0 - \gamma_0 p_0 + \frac{g}{\sqrt{\mathcal{N}}}\sum_{i=1}^{\mathcal{N}}(\sin\Theta\, p_i - \cos\Theta\, q_i)\right]dt + dW_0(t),\\
dp_i &= \left[-\omega q_i - \gamma p_i + \frac{g}{\sqrt{\mathcal{N}}}(\sin\Theta\, p_0 - \cos\Theta\, q_0)\right]dt + dW_i(t),
\end{aligned} \tag{D1}$$

where dW_i are mutually independent Wiener increments. These obey

$$\langle dW_i(t)\rangle = 0,$$
$$\langle dW_i(t) dW_j(t)\rangle = \delta_{i,j}\,\xi_i\xi_j\,dt \tag{D2}$$

with $\xi_i = \sqrt{2\gamma_i n_i(T)}$ and the occupation $n_i(T) = \frac{k_B T}{\hbar\omega_i}$ ($\gamma_{i>0} = \gamma$, $\omega_{i>0} = \omega$). To obtain the (stochastic) equation of motion for the complex amplitudes, the equations for q_i and p_i are combined again, yielding

$$d\mathbf{A} = (-i\mathcal{H}\mathbf{A} + \eta\mathbf{u})dt + i d\mathbf{W}. \tag{D3}$$

Here the vector matrix notation was extended by the Wiener-noise vector $d\mathbf{W} = (dW_0, dW_1, \dots, dW_{\mathcal{N}})^T$.

For numerical simulations, Eq. (D3) was solved numerically, by integration for randomly drawn, finite Wiener increments. More precisely, the formal solution of Eq. (D3)

$$\mathbf{A}(t) = \exp(-i\mathcal{H}t)\mathbf{A}(0) + \eta\mathbf{u}\int_0^t dt' \exp[-i\mathcal{H}(t-t')] + i\int_0^t \exp[-i\mathcal{H}(t-t')]d\mathbf{W}(t') \tag{D4}$$

is used to approximate the last integral as a sum of finite Wiener increments $\Delta\mathbf{W}$ drawn from a normal distribution with a width proportional to the square root of the step size Δt of the time discretization. By collecting the multiple random, sample paths, averages and variances are easily calculated for several quantities such as real-valued amplitudes and phase differences.

[1] C. Huygens, *Oeuvres Complètes de Christiaan Huygens* (Nijhoff, Den Haag, 1893), p. 243.
[2] C. Liu, D. R. Weaver, S. H. Strogatz, and S. M. Reppert, Cellular construction of a circadian clock: Period determination in the suprachiasmatic nuclei, Cell **91**, 855 (1997).
[3] H. G. Schuster and P. Wagner, A model for neuronal oscillations in the visual cortex, Biol. Cybern. **64**, 77 (1990).
[4] K. Wiesenfeld, P. Colet, and S. H. Strogatz, Synchronization Transitions in a Disordered Josephson Series Array, Phys. Rev. Lett. **76**, 404 (1996).
[5] J. A. Acebrón, L. L. Bonilla, C. J. Pérez Vicente, F. Ritort, and R. Spigler, The Kuramoto model: A simple paradigm for synchronization phenomena, Rev. Mod. Phys. **77**, 137 (2005).
[6] S. H. Strogatz, From Kuramoto to Crawford: Exploring the onset of synchronization in populations of coupled oscillators, Physica D **143**, 1 (2000).
[7] Y. Kuramoto, *Chemical Oscillations, Waves, and Turbulence* (Springer-Verlag, 1984).
[8] H. Sakaguchi and Y. Kuramoto, A soluble active rotater model showing phase transitions via mutual entertainment, Prog. Theor. Phys. **76**, 576 (1986).
[9] L. M. Childs and S. H. Strogatz, Stability diagram for the forced Kuramoto model, Chaos **18**, 043128 (2008).
[10] E. Ott and T. M. Antonsen, Low dimensional behavior of large systems of globally coupled oscillators, Chaos **18**, 037113 (2008).
[11] D. M. Abrams and S. H. Strogatz, Chimera States for Coupled Oscillators, Phys. Rev. Lett. **93**, 174102 (2004).
[12] D. M. Abrams, R. Mirollo, S. H. Strogatz, and D. A. Wiley, Solvable Model for Chimera States of Coupled Oscillators, Phys. Rev. Lett. **101**, 084103 (2008).
[13] C. C. Gong, C. Zheng, R. Toenjes, and A. Pikovsky, Repulsively coupled Kuramoto-Sakaguchi phase oscillators ensemble subject to common noise, Chaos **29**, 033127 (2019).
[14] C. M. Bender and S. Boettcher, Real Spectra in Non-Hermitian Hamiltonians Having $\mathcal{PT}$ Symmetry, Phys. Rev. Lett. **80**, 5243 (1998).
[15] R. El-Ganainy, K. G. Makris, M. Khajavikhan, Z. H. Musslimani, S. Rotter, and D. N. Christodoulides, Non-Hermitian physics and $\mathcal{PT}$ symmetry, Nat. Phys. **14**, 11 (2018).
[16] I. Rotter, A non-Hermitian Hamilton operator and the physics of open quantum systems, J. Phys. A: Math. Theor. **42**, 153001 (2009).
[17] N. Moiseyev, *Non-Hermitian Quantum Mechanics* (Cambridge University Press, 2011).
[18] Y.-P. Wang, J. W. Rao, Y. Yang, P.-C. Xu, Y. S. Gui, B. M. Yao, J. Q. You, and C.-M. Hu, Nonreciprocity and Unidirectional Invisibility in Cavity Magnonics, Phys. Rev. Lett. **123**, 127202 (2019).
[19] J. Schindler, A. Li, M. C. Zheng, F. M. Ellis, and T. Kottos, Experimental study of active LRC circuits with $\mathcal{PT}$ symmetries, Phys. Rev. A **84**, 040101(R) (2011).
[20] R. El-Ganainy, M. Khajavikhan, D. N. Christodoulides, and S. K. Ozdemir, The dawn of non-Hermitian optics, Commun. Phys. **2**, 37 (2019).
[21] L. Feng, R. El-Ganainy, and L. Ge, Non-Hermitian photonics based on parity–time symmetry, Nat. Photon. **11**, 752 (2017).
[22] N. R. Bernier, L. D. Tóth, A. K. Feofanov, and T. J. Kippenberg, Level attraction in a microwave optomechanical circuit, Phys. Rev. A **98**, 023841 (2018).
[23] D. Porras and S. Fernández-Lorenzo, Topological Amplification in Photonic Lattices, Phys. Rev. Lett. **122**, 143901 (2019).
[24] P. Roushan, C. Neill, A. Megrant, Y. Chen, R. Babbush, R. Barends, B. Campbell, Z. Chen, B. Chiaro, A. Dunsworth *et al.*, Chiral ground-state currents of interacting photons in a synthetic magnetic field, Nat. Phys. **13**, 146 (2017).
[25] H. P. Breuer and F. Petruccione, *The Theory of Open Quantum Systems* (Oxford University Press, 2002).
[26] D. F. Walls and G. Milburn, *Quantum Optics* (Springer-Verlag, Berlin, 2006).
[27] M. Reitz, C. Sommer, and C. Genes, Cooperative quantum phenomena in light-matter platforms, PRX Quantum **3**, 010201 (2022).